Experimental investigation of the temperature dependence of the air-gap flux density in a permanent magnet synchronous machine

János Füzesi

Óbuda University, Kálmán Kandó Faculty of Electrical Engineering, Bécsi út 94-96., 1034 Budapest, Hungary, fuzesi.janos@gmail.com

István Vajda, DSc

Óbuda University, Institute of Automation, Bécsi út 94-96., 1034 Budapest, Hungary, vajda@uni-obuda.hu

István Laczkó

A.O. Smith Hungary Kft. (former EVIG), Gyömrői út 150., 1103 Budapest, Hungary, istvan.laczko@gmail.com

The condition of the machine can be determined by diagnostic investigation of air-gap flux density in electric motors. The most practical tool for investigating magnetic fields in electric motors seems to be the Hall-cell. However, due to its size and its problematic positioning, it cannot be applied in electric machines of medium size with radial air-gap smaller than ~1 mm. The aim of the current research is the experimental investigation of the induction distribution that occurs in the air-gap, using a permanent magnet synchronous motor with increased air-gap. The prior determination of the expected parameter values took place prior to the measurement by means of finite element simulations. Based on these results, we assume that the temperature values can be calculated on the basis of the change in the air-gap induction, which is investigated by means of the currently elaborated procedure. In the experiment, a Hall-cell was positioned at a fix point of the air-gap. The measurement was carried out during rotation. The curve of points measured this way does not indicate the spatial distribution of the static air-gap induction, rather it shows the temporal change of the induction at the given measurement point. However several points of this measurements can represent the spatial distribution of the air gap magnetic field. In the series of measurements, the investigated machine was homogeneously heated in a laboratory furnace until it reached 90 Celsius degrees, while the temporal change of the induction was recorded at several measurement points. The air-gap induction decreased with the increment of the temperature. The correction of the measurement points was carried out in accordance with the temperature coefficient of the Hall voltage. The extent of changes due to the increasing temperature slightly differ from the simulation results. A possible reason for this might be the wide tolerance range of the B-H curve of the applied magnets. The aim of the research, i.e. determining the

temperature of active parts of the electric machine based on the direct measurement of the air-gap, is feasible. The future aim of the research is to improve the measurement setup by eliminating problems that negatively influence accuracy.

Keywords: air-gap, magnetic flux density, electromagnetic field analysis, temperature rise, synchronous machines, permanent magnets, Hall sensor, finite-element computations

1. Introduction

Direct measurement of magnetic flux in the air gap is a relatively new method, by means of which the rotating magnetic field can be measured in the air gap in a coordinate system fixed to the stator. Most of the papers focused on the standard industrial 3 phase asynchronous motors [1][2].

Using Hall-sensors for measurement is the best solution for economical and usability reasons. A wide range of measuring devices exists [3], but due to the relatively high measuring range (0…1 Tesla) and the required small size, the Hall-sensor is considered the best suitable tool.

The application of Hall-sensors was made possible by the fact that the size of the sensors is comparable to the radial air-gap of larger induction motors, and their price is also acceptable. Nonetheless, the size of the radial air gap of motors widely used in industry is below 0.5 mm, which is too small for direct air gap flux measurements by means of Hall-sensors available on the market.

In the experimental setup, the synchronous machine originally was a standard 3 phase industrial induction machine with aluminium squirrel cage rotor. In order to obtain more advantageous conditions for the measurements, it was modified to a permanent magnet synchronous machine. In this paper, we are introducing our first investigation, the effect of temperature rising to the permanent magnets. The question is whether we are able to determine the permanent magnets temperature parameters.

2. Methods

2.1. Introduction of the studied machine

The nominal parameters of the original induction motor prior to the modifications are shown in Table 1. This machine had a single-layer concentric winding, all the coppers has been removed.

Table 1.
Parameters of original induction machine

Induction motor: 4AM 63B 4			
Parameter		**Values**	**Units**
P_n	Rated power	0,37	kW
U_n	Nominal voltage	Δ/Y 380/220	V
I_n	Nominal current	2,08/1,20	A
n_n	Rated speed	1320	min^{-1}
$\cos\varphi_n$	Rated power factor	0,69	-
η_n	Rated efficiency	68	%
Z_1	Number of stator slots	24	-
D	Stator hole diameter	61,45	mm
l	Active length of iron core	73	mm
δ	Original radial air-gap	0,3	mm

The squirrel cage rotor had also been removed and replaced with a newly made permanent magnet rotor which is shown in Figure 1.

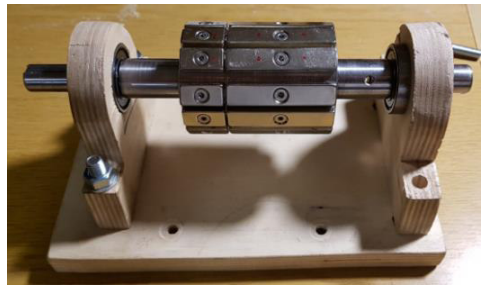

Figure 1.
New rotor with magnets

Due to some practical reasons, the motor bearing shields have been replaced to a bracket type bearing house. All physical parameters of the active parts of the motor have been measured. The new machine parameters were calculated on the basis of the article of J. Varga *et al.* [4]. In order to operate a permanent magnet

synchronous machine, it is required to use an electronic driver circuit. The driver has 24V output voltage, so the new stator parameters was determined in accordance with this requirement. Figure 2. shows the new 2 dimensional drawing of the re-designed machine.

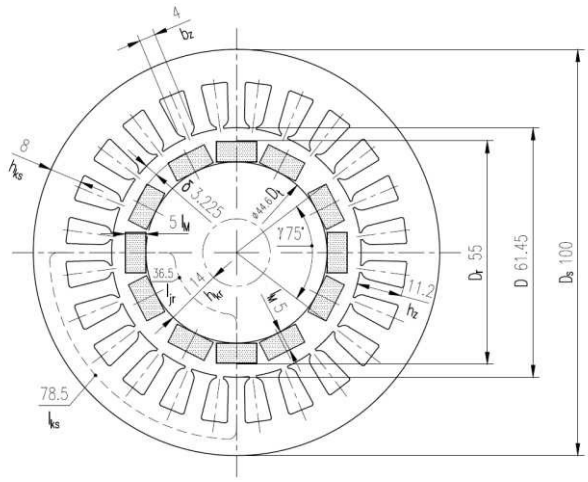

Figure 2.
Dimensional drawing of the magnetic circuit

Similarly to the original version, the synchronous machine also has a single layer concentric winding, schematically shown in Figure 3.

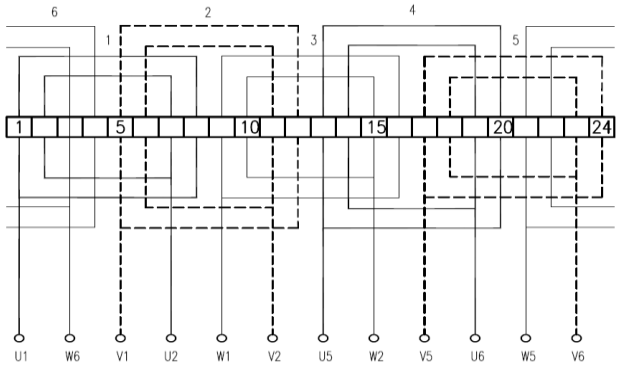

Figure 3.
Stator winding schematics

Moreover, the field in the machine has been computed by using a finite element representation in FEMM 4.2 software, shown in Figure 4.

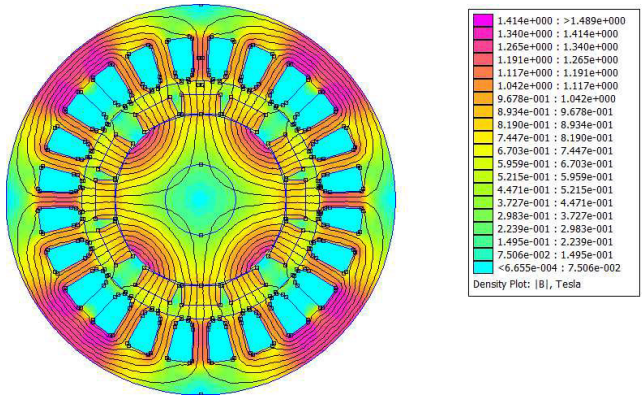

Figure 4.
Finite element simulation of the magnetic circuit

2.2. Temperature dependence of the NdFeB magnet

The temperature-dependent B-H curves of the used N48 type NdFeB magnet are illustrated in Figure 5.[5]. It can be observed that the remanence flux density decreases while the temperature is increasing. The decrementation effect is reversible until the operating point does not go beyond the knee-point of the curve which was taken into account during the calculation.

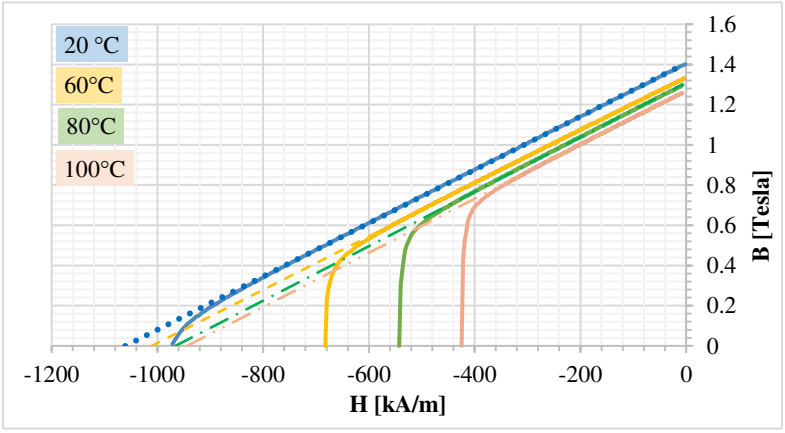

Figure 5.
Demagnetization curves of N48 type NdFeB magnet [5]

2.3. Applied Hall-sensors

In order to carry out the measurements, we used one piece of CYSJ362A GaAs Hall effect element [6] placed beneath the centre of one stator slot. This sensor has a linear U_{HALL}-B characteristic. Because of the lower thermal dependence (Figure 6.), we used 5mA constant current source for the sensor supplement. The physical sizes (2,7x2,4x0,95 mm) of the sensor are optimally small for the direct placement in the air-gap.

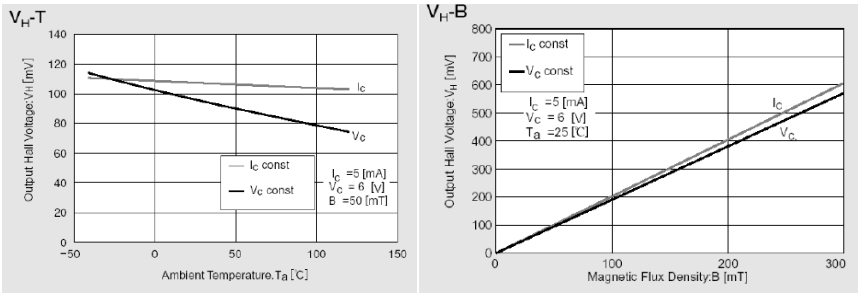

Figure 6.
Main characteristic of CYSJ362A GaAs Hall sensor [6]

2.4. Predictions of the FEMM simulation

In the FEMM model we also represented the Hall cell by a 1mm line marked with the red rectangle in Figure 7. The average flux density along this line can be obtained from FEMM.

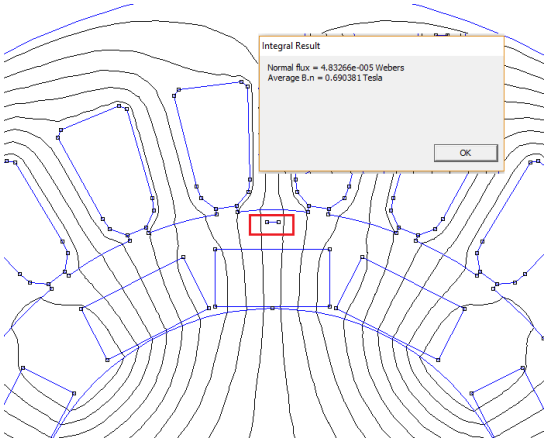

Figure 7.
Sensor placement and modelling in FEMM

In FEMM software environment, the LUA script language allows the rotation to be simulated. One hundred steps have been added to a text file in 1-degree increments. To take the temperature rise into consideration, the permanent magnet's different B-H curves can be adjusted in FEMM according to Figure 5. The simulation result for 100 steps in 20 and 80° Celsius degree is shown in Figure 8. According to the thermal dependent B-H curves, a smaller flux density belongs to the same coercive force at higher temperature. The difference between the two peak value is 7,68 percent.

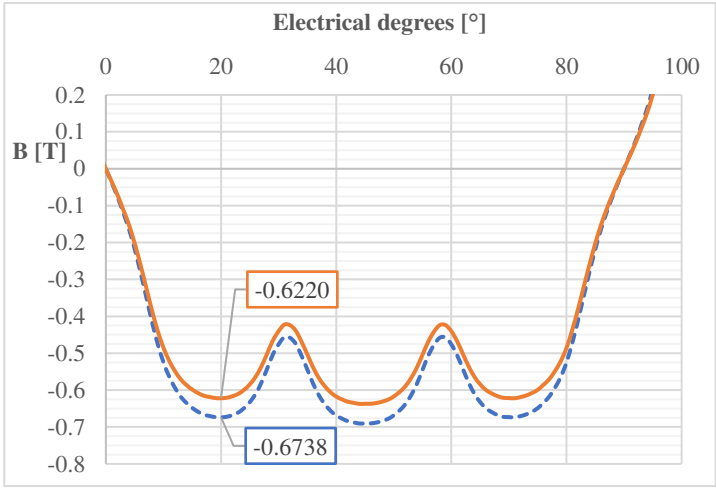

Figure 8.
Temporal change of the induction at the given measurement point

2.5. Experimental setup

To reach the requested temperature of the motor, a laboratory furnace was used. The furnace was sufficiently large so that the entire experimental setup could placed in it, Figure 9. One Pt100 platinum resistance thermometer placed inside of the motor. Our starting point was our assumption that if the temperature rising of the overall motor reaches the maximum point then the temperature of all parts will be equal, including the magnets.

Figure 9.
Experimental set with sensors inside of the furnace

After 2 hours, the temperature stabilised at 90° Celsius degree. During the heating procedure, the motor was rotated, and the parameters were monitored.

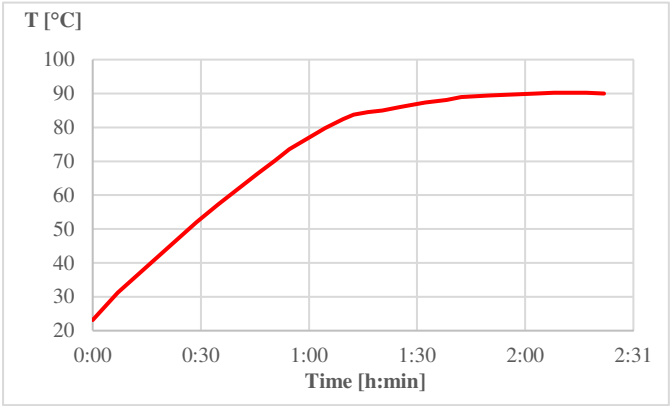

Figure 10.
Temperature rising curve, measured by Pt100

3. Results and discussion

The first measuring point was at 23,14°C ambient room temperature. At this point, a screenshot was taken from the oscilloscope (shown in Figure 11.) The Y-axis represents the directly the sensor Hall-voltage.

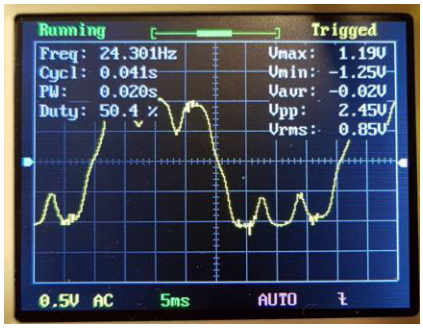

Figure 11.
Oscilloscope screenshot at starting temperature point

The rotating speed was 729 min^{-1}. The rotating speed can be calculated form the measured frequency (1).

$$f = \frac{n \cdot p}{60} \rightarrow n = \frac{f \cdot 60}{p} = \frac{24{,}301 \cdot 60}{2} = 729{,}03\ min^{-1} \quad (1)$$

where f, frequency in Hz, n, rotating speed in min^{-1}, p the number of poles.

The signal shown in Figure 11. has several needle pulses. These pikes are not due to the magnetic field in the air-gap rather these are caused by EMC effects of driver circuit.

The final measuring point, at thermal equilibrium, was measured after 2 hours at 89,96°Celsius degree. According to the oscilloscope screenshot in Figure 12, the magnetic flux density in the air-gap decreased in accordance with the prediction of the theory.

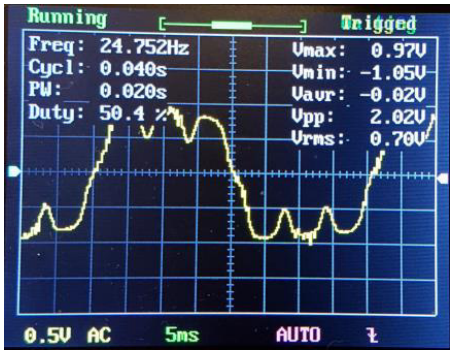

Figure 12.
Oscilloscope screenshot at thermal equilibrium point

The summary of results of hot and cold state measurements are shown in Figure 15. The measured Hall voltages were converted into magnetic flux values.

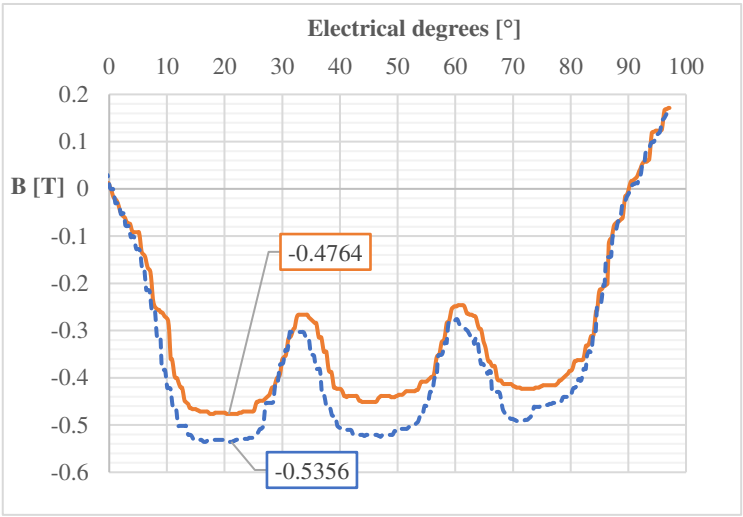

Figure 13.
Summary of results

Between the cold and the hot state, the temperature difference is ΔT=66,82K. The reduction was found to be ~12,7%.

Conclusions

It is obvious that the temperature rise caused significant drop of the air-gap flux density, however, by means of appropriate measurements and calibration, the temperature of the magnets can be obtained without physical contact of the magnet surface.

Experimental results are in accordance with the FEMM simulation. Minor differences between FEMM simulation and test results are caused by the uncertainty of the magnet characteristics.

Obviously, more than just one sensor is needed for accurate investigation of the spatial distribution of air gap flux density. Future work should be carried out in this direction.

Acknowledgement

This research has been partly supported by “GINOP-2.3.4-15-2016-00003” for Higher Education and Industrial Cooperation Centre in Győr.

References

[1] K. Saad and G. Mirzaeva, “Fault diagnosis of induction motors by space harmonics analysis of the main air gap flux,” *Proc. - 2014 Int. Conf. Electr. Mach. ICEM 2014*, no. September 2014, pp. 1608–1613, 2014.

[2] V. Kindl, K. Hruska, J. Sobra, and M. Byrtus, “Effect of induction machine’s load and rotor eccentricity on space harmonics in the air gap magnetic flux density,” in *Proceedings of the 16th International Conference on Mechatronics, Mechatronika 2014*, 2014, no. December, pp. 463–468.

[3] J. E. Lenz, “A Review of Magnetic Sensors,” *Proc. IEEE*, vol. 78, no. 6, pp. 973–989, 1990.

[4] D. Basic and J. Varga, “Permanens felületmágneses forgórészű szinkron szervomotorok tervezésének irányelvei,” *Villamosság*, vol. 39. évf., no. 9. szám, pp. 257–288, 1991.

[5] Arnold Magnetics, “Neodymium Magnets (NdFeB) | Arnold Magnetic Technologies.” [Online]. Available: http://www.arnoldmagnetics.com/products/neodymium-iron-boron-magnets/. [Accessed: 12-May-2018].

[6] ChenYang Gmbh, “Hall effect sensor CYSJ362A Datasheet,” vol. 49, no. 0, pp. 0–3, 2016.